



Comparison and selection of ground motion prediction equations for the Sichuan–Yunnan area, southwest China

Jingwei Liu^{1,2} · John Douglas²

Received: 17 October 2023 / Accepted: 7 January 2024 / Published online: 1 February 2024
© The Author(s) 2024

Abstract

The Sichuan–Yunnan area is one of the most seismically active regions in China. As ground-motion models form a key component of seismic hazard analysis, it is important to select (or develop) appropriate models for this area. The increasing number of digital ground-motion records of earthquakes in this area has allowed the development of local ground motion prediction equations (GMPEs). This study compares and, later, recommends appropriate GMPEs for the Sichuan–Yunnan area. We first evaluate the inherent quality of local GMPEs, with respect to their underlying datasets, the variables used and their functional forms, to determine a set of candidate GMPEs. Then we investigate how well the predictions from the GMPEs match observations computed from strong-motion records of recent earthquakes in this area. The fit between predictions and observations varies significantly amongst the GMPEs. The results suggest that some recent local GMPEs would lead to biased ground-motion estimates due to limitations of their underlying datasets and functional forms. Based on both evaluations of inherent quality and compatibility with observations, only one local GMPE is recommended. A comparison of the predictions from three widely-used non-local GMPEs indicates that ground motions in the Sichuan–Yunnan area appear more variable than those in other regions but that predictions from these non-local GMPEs are generally unbiased. We recommend use of a mixture of robust local and non-local GMPEs within seismic hazard analyses to capture the epistemic uncertainty in ground-motion prediction for this area.

Keywords Ground-motion models (GMMs) · Predictions and observations · Ground-motion records · Residual analysis · Epistemic uncertainty · Seismic hazard assessment

✉ John Douglas
john.douglas@strath.ac.uk

¹ National Institute of Natural Hazards, Ministry of Emergency Management of China, Beijing 100085, China

² Department of Civil and Environmental Engineering, University of Strathclyde, James Weir Building, 75 Montrose Street, Glasgow G1 1XJ, UK

1 Introduction

The area comprising the provinces of Sichuan and Yunnan, which are located near the south-eastern boundary of the Tibetan plateau, is one of the most tectonically and seismically active regions in China. Since the beginning of the historical record (~800 C.E.), two massive earthquakes ($M_S \geq 8.0$), the 1833 Songming earthquake in 1833 and the 2008 Wenchuan (WC) earthquake, and approximately 40 large earthquakes ($7.0 \leq M_S \leq 7.9$) have occurred in this area. More than 130 million people in the Sichuan–Yunnan area thus face high seismic hazard and, given the vulnerability of the structures in the area, high risk.

Ground-motion models (GMMs), including both empirical (i.e. those based on regression of observed ground motions) models and those derived using physics-based approaches, are a crucial component of seismic hazard analysis. Such models should capture “the centre, the body, and the range” (viz. the guidelines of the Senior Seismic Hazard Analysis Committee, SSHAC) of future earthquake ground motions either by using a suite of GMPEs or through a backbone approach (e.g., Douglas 2018). The most widely-used GMMs are ground motion prediction equations (GMPEs), which are generally derived through regression analysis of empirical data. In the following we use “GMM” to refer to a suite of GMPEs to capture the epistemic uncertainty in ground-motion prediction.

Due to a sparsity of digital ground-motion records from China, Hu and Zhang (1984) introduced the transform method in the 1980s to derive GMPEs for peak ground acceleration (PGA) and response (pseudo) spectral accelerations (PSAs). This approach was widely used in China subsequently (e.g., Huo 1989; Wang et al. 2000; Yu 2002). The GMPEs most widely used for seismic hazard analysis of major engineering projects are still based on the transform method, like the models by Xiao (2011) and China Earthquake Administration (2019) (hereafter, CEA 2019). In this method, a reference area with abundant instrumental ground-motion records and macroseismic intensities (e.g., the western United States of America, USA) is chosen. Then separate GMPEs to predict PGA or PSA and macroseismic intensities are derived for the reference area and a similar GMPE for macroseismic intensity for the target area (in our case, China). The assumption then made is that, for the same magnitude and distance, the same level of macroseismic intensity in both areas would correspond to the same level of PGA or PSA. This then allows a GMPE for PGA or PSA to be estimated for the target area by converting between macroseismic intensity and PGA or PSA. While the transform method has obvious imperfections, e.g., large intervals between intensity values, this method is commonly used. The method has highlighted that ground-motion characteristics vary amongst Chinese regions (Yu and Wang 2004, 2006; Zhao et al. 2009; Fan et al. 2011).

More and more ground-motion records have been collected in China with improvements in strong-motion networks since the early 2000s, especially in the Sichuan–Yunnan area. This increasing number of records facilitates the development of local GMPEs. Various GMPEs have been derived directly from local ground-motion records from the Sichuan–Yunnan area: Cui et al. (2012), Wang et al. (2013), Li et al. (2020) for PGA and PSAs and Fan et al. (2020) and Zhang et al. (2021) for peak ground velocity (PGV) and peak ground displacement. The development of these GMPEs does not just indicate great progress for regional seismic hazard analysis but also provides more choices of GMPEs for such analyses. Given the complex regional characteristics of ground motions, it is not evident that GMPEs derived using data from other regions (e.g., western USA) are well calibrated to the characteristics of a target region (here, Sichuan–Yunnan) in terms of its source and path properties (e.g., Bommer and Stafford 2020). Region-specific GMPEs

could show more consistency with the records from the target region than other models as long as the region-specific GMPEs satisfy the requirements of seismic hazard analysis (e.g., Mousavi et al. 2012; Ghasemi and Allen 2022). Therefore, region-specific GMMs are generally recommended for a specific site/region as GMMs vary from region to region, because of differences in, e.g., source characteristics, path effects related to geometric spreading and anelastic attenuation (e.g., Cotton et al. 2006; Goulet et al. 2018; Weatherill et al. 2020).

To develop appropriate GMMs, GMPEs need to be evaluated against their potential performance in predicting ground motions for the target area and requirements for probabilistic seismic hazard analyses (e.g., Bommer et al. 2010). For the purposes of site-specific, national or continental hazard analyses, candidate GMPEs have been evaluated in many studies, e.g., for the USA (e.g. Abrahamson et al. 2008; Gregor et al. 2022; McNamara et al. 2019), for Australia (e.g. Ghasemi and Allen 2022), for Italy (e.g. Lanzano et al. 2020), for Europe and the Middle East (e.g. Stafford et al. 2008; Campbell and Bozorgnia 2006; Campbell 2016) and globally (e.g. Stewart et al. 2015). Very few studies have undertaken such an evaluation for China. Huang and Galasso (2019) compared the NGA-West2 GMPEs and one local GMPE to local ground-motion records in the Sichuan province. Despite this study's interesting finding that ground motions in this province are characterized by slower attenuation than modelled by the NGA-West2 GMPEs, this study was based on only a single local candidate GMPE and relatively few ground-motion records. The local GMPE (Huo 1989) used in their comparison was developed more than 30 years ago using the transform method, which does not correctly model recent ground-motion observations (Wang 2010). Besides, the ground-motion records used by Huang and Galasso (2019) came from only three recent strong earthquakes, which are not necessarily typical of ground motions in the Sichuan province, especially since relatively small and moderate earthquakes have caused significant damage in this area.

In this study, we evaluate GMPEs to recommend appropriate models for the Sichuan–Yunnan area. First, we compile all regional GMPEs derived from local instrumental ground-motion records. Second, these candidate GMPEs are evaluated based on their datasets, functional forms and independent variables, the methods used to derive the models, and the range of response periods considered. Next, we compare predictions from the candidate GMPEs to local ground-motion records by computing inter- and intra-event residuals (also known as between- and within-event residuals). Finally, we make some recommendations of appropriate GMPEs for use within seismic hazard analyses of the Sichuan–Yunnan area.

2 Determination of candidate GMPEs

We searched for all published GMMs developed for the Sichuan–Yunnan area and identified 14 candidate GMPEs. This excludes models derived for specific sites or from single earthquakes only. In addition, we have only considered GMPEs that have used data from a wide range of magnitudes because these have wider applicability. Therefore, those GMPEs that have used data from small and moderate earthquakes only are not included in our comparisons. This includes the GMPE of Jiang (2017).

Huo (1989), Yu and Wang (2006) and Lei et al. (2007) derived their GMPEs using the transform method. These models assume elliptic attenuation because isoseismal maps usually use elliptic contours to describe the effects of an earthquake. It is difficult, however,

to estimate the major axes of future earthquakes as the strikes of faults vary. This creates a difficulty and uncertainty when predicting ground motions for future events. Given the problems discussed above with the transform method and these difficulties with assuming elliptic attenuation, these GMPEs have been excluded from the following evaluation.

The GMPEs of Xiao (2011) and CEA (2019) are also derived using the transform method, although the ground-motion records of the WC earthquake were included during the regression analysis. In addition, they both assume elliptic attenuation, which makes them more difficult to use. As mentioned above, however, they are the most widely used GMPEs within seismic hazard analyses for major engineering projects in China. Because of this and despite the potential difficulties in applying them, the GMPEs of Xiao (2011) and CEA (2019) are considered in the later residual analysis.

Eight other Sichuan–Yunnan GMPEs derived using the standard method of regression on ground-motion data (and not the transform method) are considered more carefully in the following. These are the models of: Cui et al. (2006), Kang and Jin (2009), Cui et al. (2012), Wang et al. (2013), Zhang et al. (2013), Wen et al. (2018), Li et al. (2020), and Zhang et al. (2022). These eight GMPEs were developed for Sichuan and/or Yunnan using local ground-motion data. Most of them were published in peer-reviewed journals except Cui et al. (2012), which is a conference paper, and all of them have not yet been superseded by a new article by the same authors. Thus, none of models can be excluded by basic quality assurance criteria without looking deeper.

Following exclusion criteria suggested by Bommer et al. (2010) for GMPEs of shallow crustal earthquakes, the main elements used for the assessment of the GMPEs applicability are: the dataset used, the range of response periods, the functional form and the independent variables, the methods used to derive the coefficients, and the magnitude and distance ranges of applicability. These are discussed in turn in the following sections.

2.1 Dataset selection

All datasets used to derive these GMPEs consist of instrumental ground motions of earthquakes that occurred in the Sichuan–Yunnan area. Zhang et al. (2013) and Li et al. (2020) also used a small number of ground-motion records from global shallow crustal earthquakes. Each group of authors developed their own selection criteria for records, including considerations of the magnitude and distance ranges, the minimum and maximum number of records for each event, the numbers of components considered and how they were combined, recording quality criteria and whether records from aftershocks were included.

Details are listed in Table 1. It is obvious that Cui et al. (2006) provides limited details on the dataset used. Kang and Jin (2009) did not provide sufficient information on their dataset either. In addition, they only used records from aftershocks of the WC earthquake (from 12th May to 10th June 2008). It is debatable if one specific earthquake sequence is sufficient to derive a widely applicable GMPE. The rest of the considered GMPEs were derived from records of moderate and strong earthquakes ($M \geq 4.0$), and the number of records from each earthquake should be sufficient for regression analysis.

In summary, all eight studies collated their own datasets of instrumental records and used them to derive GMPEs according to their own selection criteria, but the quality of the datasets varies considerably. Based on the characteristics of datasets discussed above, the GMPEs of Cui et al. (2006) and Kang and Jin (2009) would be excluded at the first step as it is likely that these models will be unreliable due to inadequacies of their datasets. In the

Table 1 Characteristics of records and selection criteria used by the GMPE developers

GMPE	Num-ber of records	Number of earthquakes	Average number of records per earthquake	Time range of records	Minimum num-ber of records per earthquake	Maximum num-ber of records per earthquake	Selection criteria		Components
							Magnitude range	Distance range (km)	
Cui et al. (2006)	248	≥ 9	≤ 24.8	1985–2001	N/A	N/A	N/A	N/A	H + V
Kang and Jin (2009)	8505	105 (only after-shocks of WC earthquake)	81	12/05/2008–10/06/2008	N/A	N/A	$3.0 \leq M_w \leq 6.4$	$26 \leq R_{epi} \leq 462$	H
Cui et al. (2012)	962	7	137.4	06/2007–05/2008	10	837 (WC Earth-quake)	$M_S \geq 4.5$	$R_{epi} < 110$	H
Wang et al. (2013)	951	90	10.6	2007–2008	17 for main shock (unknown for aftershocks of WC)	64 for main shock (unknown for aftershocks of WC)	$4.5 \leq M_S \leq 6.5$	$R_{rup} \leq 200$	H
Zhang et al. (2013)	1315	39 (WC and 18 aftershocks, 20 global earth-quake)	33.7	05/2008–08/2008 (local) 1966–1999 (global)	3	343	$5.0 \leq M_S \leq 8.0$	200	H
Wen et al. (2018)	1644	186	8.8	12/2007–12/2015	4	N/A	$4.0 \leq M_S \leq 6.7$	$2 \leq R_{jg} \leq 200$	H
Li et al. (2020)	526	4	35.7 (local) 12.5 (global)	05/2008–10/2014 (local) 1952–2009 (global)	16 (local) 1 (global)	70 (local) 60 (global)	$6.0 \leq M_w \leq 7.9$ (local) $6.1 \leq M_w \leq 7.68$ (global)	$R_{rup} \leq 200$	H
Zhang et al. (2022)	1324	70	18.9	06/2007–09/2018	3	119	$4.2 \leq M_w \leq 7.9$	$0 < R_{rup} < 300$	H

following only the six remaining models: Cui et al. (2012), Wang et al. (2013), Zhang et al. (2013), Wen et al. (2018), Li et al. (2020), and Zhang et al. (2022), are considered.

2.2 Function form and variables

As shown in Table 2, all the GMPEs use logarithmic functions, with magnitude, distance, site and style-of-faulting terms. The logarithmic form of GMPEs is justified as the distribution of ground motion parameters has been shown to follow a lognormal distribution, except potentially for very high amplitude motions. The ground motion parameters (PGA, PGV, and 5%-damped PSA) are non-linear functions of magnitude and source-to-site distance. Neither epicentral distance, R_{epi} , nor local magnitude, M_L , are generally appropriate variables to predict ground motions of moderate and large earthquakes, particularly within the near-source region. Site-effect terms that are not in terms of the time-average shear-wave velocity to 30m, V_{S30} , or another physical measurement would likely not be optimum either. This indicates that the GMPEs of Cui et al. (2012) and Wang et al. (2013) would be less suitable than others, which use appropriate magnitude and distance scales and even consider style-of-faulting effects in their functions.

2.3 Derivation method

Since all functional forms of GMPEs are logarithmic, it is important to choose a regression method that accounts for inter- and intra-event components of variability when deriving the coefficients of a GMPE (e.g. Douglas 2003). The intra-event effects include systematic bedrock or site-specific effects and path-specific effects, and the inter-event component contains systematic source-specific effects (Al Atik et al. 2010). Table 3 lists the methods used by their developers to derive the candidate GMPEs, for their residual analyses (if performed) and to test the resulting GMPEs. Some of the developers calculated inter- and intra-event residuals. Most of the developers tested their GMPEs by comparing them with previous models and/or with observed ground-motion data, which adds credibility to the GMPEs.

For each of the candidate GMPEs, we evaluated the predicted PGA curves against distance. These curves exhibit similar and reasonable shapes, except the curves from the GMPE of Wen et al. (2018). As shown in Fig. 1a, as well as the very small values of PGA (in terms of an unknown unit), the curves are inappropriate because predictions for $M_w = 5.0$ are greater than those for $M_w = 8$. Examining the coefficients carefully, it was noticed that the values of a_2 and a_4 (from Table 1 in Wen et al. 2018) were unusual with positive and negative values, respectively, when they would be expected to be negative and positive. To check for a simple clerical error, we switched the values for a_2 and a_4 , and then redrew the PGA curves for various magnitudes. Comparing these new curves with the original ones, the values of PGA in Fig. 1b are now much too high and the shapes of the curves are unusual. When examining the unit covariance matrix, Wen et al. (2018) themselves highlight that some of the coefficients of their GMPEs (including those related to the magnitude scaling) show strong trade-offs, which they relate to their data's relatively narrow magnitude range and few near-source records. Therefore, the GMPE of Wen et al. (2018) is rejected from further comparisons.

Therefore, there are five models left for the following comparison: Cui et al. (2012), Wang et al. (2013), Zhang et al. (2013), Li et al. (2020) and Zhang et al. (2022).

Table 2 Functional forms, the variables used and their ranges of applicability of the considered GMPEs

GMPE	Functional form	M scale	R scale	Site effects	Other source effects	Range of applicability		Notation
						M	R (km)	
Cui et al. (2012)*	$\log Y = c_1 + c_2 M_S + c_3 \log (R_{epi} + R_0) + c_4 S$	M_S	R_{epi}	Site factor S	N/A	N/A	N/A	R_0 is a near-field saturation factor
Wang et al. (2013)#	$\log Y = c_1 + c_2 M_S + c_3 M_S^2 + (C_4 + C_5 M_S) \times \log [R_{rup} + C_6 \exp (C_7 M_S)]$	M_S	R_{rup}	N/A	N/A	uncertain	uncertain	
Zhang et al. (2013)	$\ln Y = f_B (M_S, R_{rup}) + b_1 SS + b_2 RS + b_3 NS + f_{site} (V_{S30}) + F_{HW} / f_{HW} (M_S, R_{rup})$	M_S	R_{rup}	V_{S30}	Style-of-faulting and hanging-wall term f_{HW}	$M_S \geq 5.0$	$R_{rup} \leq 200$	SS, RS, NS refers to strike-slip, reverse and normal faulting, respectively
Wen et al. (2018)	$\ln Y = a_1 + a_2 M_S + a_3 \ln (R_{JB} + a_4 M_S) + a_5 R_{JB} + a_6 \ln (V_{S30})$	M_S	R_{JB}	V_{S30}	N/A	$M_w > 4.0$	$R_{JB} \leq 200$	
Li et al. (2020)	$\ln Y = b_1 M_w^2 + b_2 M_w + b_3 M_w \ln R_{rup} + b_4 \ln R_{rup} + f_{mech} + f_{site} + F_{HW} / f_{HW} (M_w) / f_{HW} (R_{rup})$	M_w	R_{rup}	V_{S30}	Style-of-faulting term f_{mech}	$M_w > 6.0$	$R_{rup} \leq 200$	
Zhang et al. (2022)	$\ln Y = f_{mag} (M_w) + f_{ds} (M_w, R_{rup}) + f_B (Z_{TOR}) + f_{mag} (M_w, R_{rup}, Z_{TOR}, \delta) + f_{site} (V_{S30}) + f_{att} (R_{rup})$	M_w	R_{rup}	V_{S30}	Style-of-faulting term f_B , hanging-wall term f_{mag}	$4.2 \leq M_w$	$10 \leq R_{rup} \leq 200$	Z_{TOR} indicates the depth to the top of the coseismic rupture

*To compare and analyse the influence of WC aftershock data, Cui et al. (2012) performed (a) unweighted regression for all data and (b) weighted regression except for the WC aftershock data, and presented coefficients for each regression. The sub-models of Cui et al. (2012) are expressed as Cui2012_weighted and Cui2012_unweighted in the subsequent text and figures

#To consider the effect of geometric characteristics of the source-to-site azimuth, Zhang et al. (2013) rotated the horizontal component of ground motions into two sub-components: parallel to the fault strike (FP) and perpendicular to the fault strike (FN), so Zhang et al. (2013) has FP and FN sub-models, denoted as Zhang2013_FP and Zhang2013_FN in the subsequent text and figures

Table 3 Methods used by the GMPE developers

GMPE	Methods	Residual evaluation	Results test	Range of standard deviation (in terms of natural logarithms)		
				Total	Inter-event	Intra-event
Cui et al. (2012)	Genetic hybrid algorithm combining genetic algorithm and nonlinear unconstrained least-square optimization	Total residual error	Compared with their own previous models	0.649–0.256 (unweighted) 0.755–0.967 (weighted)	N/A	N/A
Wang et al. (2013)	Linear regression and nonlinear fitting	N/A	Compared with one previous model	0.665–0.944	N/A	N/A
Zhang et al. (2013)	Random-effects regression (Abrahamson and Youngs 1992)	N/A	Compared with observations and NGA models	0.577–0.830 (FP) 0.583–0.831 (FN)	0.269–0.535 (FP) 0.287–0.519 (FN)	0.511–0.657 (FP) 0.507–0.648 (FN)
Wen et al. (2018)	Random-effects regression (Abrahamson and Youngs 1992)	Inter- and intra-event standard deviations, total standard deviations, unit covariance values of any two coefficients, single-station standard deviation	N/A	0.666–0.862	0.350–0.438	0.567–0.742
Li et al. (2020)	Regression analysis without further details	Inter- and intra-event residuals	Compared with NGA-Wes2 models and other models	0.667–0.890	0.333–0.663	0.540–0.682
Zhang et al. (2022)	Standard regression analysis	Inter- and intra-event residuals	Compared with observations and other models	0.671–0.941	0.494–0.755	0.419–0.570

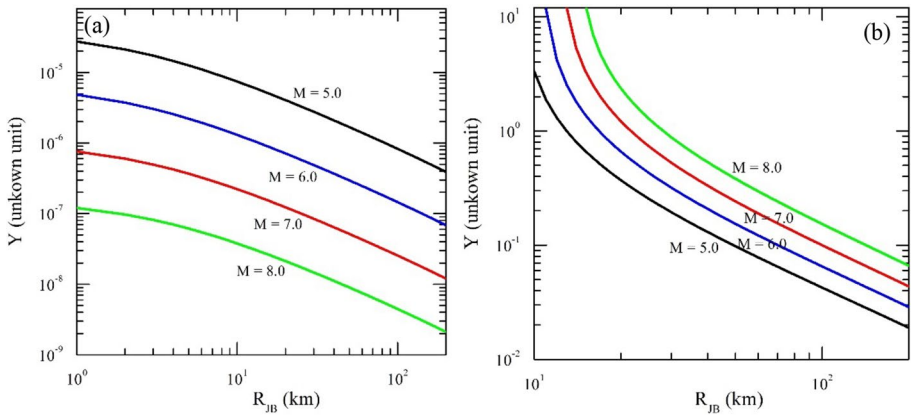


Fig. 1 a Attenuation of PGA for magnitude 5.0, 6.0, 7.0 and 8.0 using the GMPE of Wen et al. (2018). b Using the published equation but switching the values of a_2 and a_4

2.4 Range of response periods

GMMs should provide predictions for a wide range of response spectral periods (from 0s, i.e., PGA, up to at least 2 s) (Bommer et al. 2010). According to the requirements of Chinese code for seismic design of buildings (MHUDPRC 2010), response spectral periods up to 6s are required from seismic hazard analyses. As shown in Fig. 2, all five

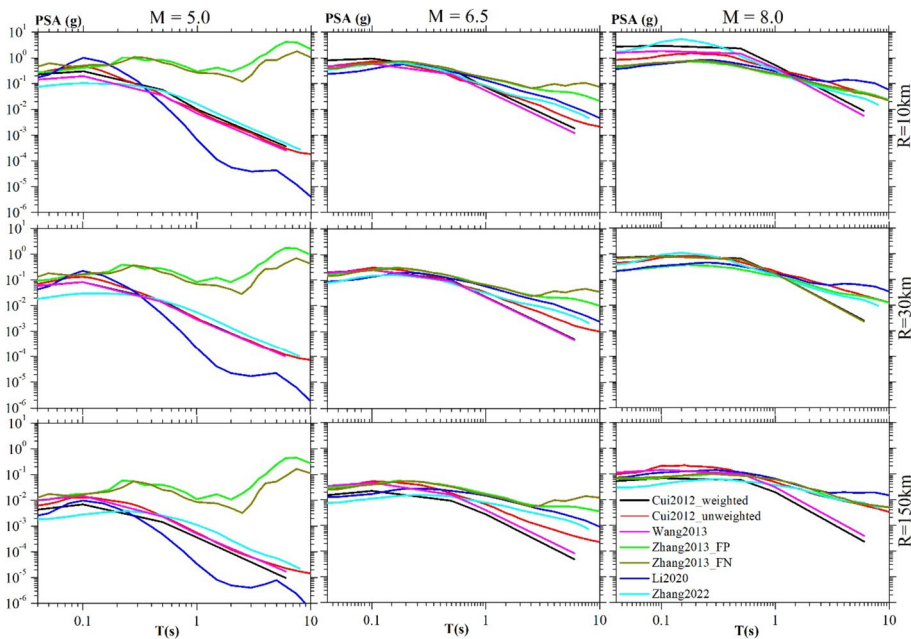


Fig. 2 Comparison of predicted response spectra from candidate GMPEs for various magnitudes and distances assuming rock site conditions, and assuming strike-slip faulting and a footwall site (if applicable)

remaining GMPEs provide predictions from 0.0 to at least 6.0s, although the number of sampling points varies from model to model. For the GMPE of Cui et al. (2012), the sampling points are too spread out to enable smooth response spectra to be drawn, while the other four GMPEs generate smoother spectra. Most spectra show large variations at longer periods (beyond 6s), probably due to noise in the ground-motion data and a limited records being used at such periods. The GMPEs of Zhang et al. (2013) and Li et al. (2020) show unusual behaviour for smaller earthquakes. These unusual predictions were confirmed by comparing them against spectra shown in the original articles.

Despite the above-mentioned weaknesses of these GMPEs, all GMPEs predict similar levels of ground motion for common response periods (Fig. 2). These equations appear to provide reasonable and similar predictions of PSA up to around 2 s. Overall, the GMPEs of Wang et al. (2013) and Zhang et al. (2022) provide better predictions for the whole period range, with the PSAs from Zhang et al. (2022) showing less variation with period than those from Wang et al. (2013).

2.5 Conclusions of this GMPE evaluation

Through looking at each aspect of the candidate GMPEs, we were able to understand the inherent quality of each GMPE in terms of their datasets, functional forms, independent variables and the magnitude and distance ranges of their applicability. A summary of these findings are reported below.

- There is no detailed accessible list of records or the detailed characteristics of the database used by Cui et al. (2006) or Kang and Jin (2009), which makes it harder to assess the reliability and applicability of these GMPEs. Therefore, both these GMPEs were excluded before any detailed comparison was carried out.
- Cui et al. (2012) mainly used observational data from the mountainous area of the Sichuan–Yunnan area, and hence the GMPE from Cui et al. (2012) may be applicable for seismic hazard analysis in this area. The specific magnitude and distance ranges of applicability of this GMPE are also unknown. In addition, the GMPE's use of epicentral distance means that it is likely unreliable in the near-source region of moderate and large earthquakes. Similarly, V_{S30} was not considered when modelling local site effects. Overall, this GMPE is not considered appropriate for most seismic hazard assessments.
- Wang et al. (2013) did not consider V_{S30} for the site terms of their GMPE either. This GMPE also has a narrow magnitude range of applicability due to the data used ($4.5 \leq M_S \leq 6.5$). In consequence, this GMPE is also not considered appropriate for most seismic hazard assessments.
- As stated in their article, the GMPE from Zhang et al. (2013) could be used to predict ground motions for earthquakes of magnitude equal to and greater than 5.0 within a rupture distance of 200 km. The applicability of this model for moderate earthquakes is, however, doubtful as we do not obtain reasonable response spectra for earthquakes of magnitude 5 using this GMPE.
- According to the range of magnitude and distance indicated by Wen et al. (2018), their GMPE is applicable for $M_w > 4.0$ and within a Joyner–Boore distance of around 200 km. The coefficients provided in this article, however, are likely incorrect because of the unusual ground-motion predictions they generate.

- As discussed above, the GMPE of Li et al. (2020) could be appropriate for the prediction of horizontal PGA and PSAs of strong ($M > 6$) earthquakes within a rupture distance of 200 km.
- Zhang et al. (2022) stated that their GMPE showed good performance for estimating PSAs from earthquakes with M_w 4.2–7.9 and rupture distances from 10 to 200 km, at sites with $V_{S30} = 140$ –1130 m/s. The predicted response spectra shown here confirmed this good performance.

In conclusion, we assessed these eight candidate GMPEs by following the Bommer et al. (2010) exclusion criteria. As listed in Table 4, the GMPE from Zhang et al. (2022) is the only one that passes all Bommer et al.'s basic exclusion criteria. Wen et al. (2018) may pass if the correct coefficients were available. In addition, Li et al. (2020) could be an appropriate choice if the focus was only on calculating ground motions from earthquakes with $M > 6$.

3 Comparisons of GMPEs to local ground-motion records

To further evaluate the performance of these models, we compared predictions from the five remaining GMPEs to local ground-motion data. Various studies have used goodness-of-fit measures such as the mean and standard deviations of the residuals, log-likelihood and Euclidean distances to assess the match between observations and predictions for different regions (e.g. Scherbaum et al. 2004, 2009; Kale and Akkar 2013; Mousavi et al. 2014). These measures capture the overall fit between the observations and predictions within a handful of values and hence they are useful data reduction methods, especially when ranking many GMPEs. We have decided not to rank the GMPEs based on these measures as we believe that presenting plots of observations and predictions, and graphs showing inter- and intra-event residuals (as well as computing the bias and standard deviations, as well as best-fit trends, from these residuals) provides a more complete description of where the GMPEs fit the data. Our approach is similar to that taken by, for example, Scasserra et al. (2009) for Italy.

3.1 Database of ground-motion records

All instrumental data used in this study are provided by the Strong Motion Observation Centre within the Institute of Engineering Mechanics of the China Earthquake Administration (hereafter SMOC). The official data that are available from SMOC start in 2007 and currently end in 2017. The database contains source parameters (epicentre locations, hypocentral depths and magnitudes), station parameters (station locations and basic site conditions) and ground-motion values (PGA and PSAs for various spectral periods). The records are from 946 earthquakes that occurred in the Sichuan–Yunnan area between January 2007 and December 2017.

The magnitudes provided were either on the surface-wave or local scales, so to be consistent with the magnitude scale used in most of the candidate GMPEs, moment magnitudes M_w were collected from the Global Centroid-Moment-Tensor (GCMT) catalogue when available or from the M_w -based earthquake catalogue for China compiled by Cheng et al. (2017). Based on three Chinese earthquake catalogues and three global M_w catalogues (GCMT, ISC-GEM and NEIC), Cheng et al. (2017) compared events with M_S in Chinese

Table 4 Overall assessment of the five remaining GMPEs according to Bommer et al. (2010)'s exclusion criteria

Bommer et al. (2010)'s exclusion criteria	Cui et al. (2012)	Wang et al. (2013)	Zhang et al. (2013)	Li et al. (2020)	Zhang et al. (2022)
1. Inappropriate tectonic environment	×	×	×	×	×
2. Not published in a peer-reviewed journal	√	×	×	×	×
3. Did not present an accessible dataset	×	×	×	×	×
4. Superseded by a more recent publication	×	×	×	×	×
5. Does not provide spectral predictions for an adequate range of response periods from 0.0 to 2.0 s	×	×	×	×	×
6. The functional form lacks either non-linear magnitude dependence or magnitude-dependent decay with distance	×	×	×	×	×
7. The coefficients of the model were not determined with a method that accounts for inter- and intra-event components of variability	√	√	√	×	×
8. Inappropriate definitions for explanatory variables	√	√	×	×	×
9. The range of applicability of the model is too small to be useful for PSHA: $M_{\min} > 5, M_{\max} < 7, R_{\max} < 80$ km	√	√	√	√	×
10. Model constrained with insufficiently large dataset	×	×	×	×	×

A cross indicates that it is not excluded by the criteria and a tick indicates that is excluded

earthquake catalogues with M_w in global catalogues and then derived M_S – M_w regression relationships using a constrained general orthogonal regression method. These relationships were used to estimate M_w for the earthquakes without an entry in the GCMT catalogue.

Considering the magnitude range of applicability of these GMPEs listed in Table 1, we selected ground-motion records from earthquakes of $M_w \geq 4.8$. This leads to 3,279 records from 71 mainshocks of M_w 4.8–7.9. The locations of these earthquakes are shown in Fig. 3. The WC earthquake of 2008 generated a large sequence of aftershocks, including some strong earthquakes. Therefore, we have included those records in the following comparison (1,756 records from 58 aftershocks of the WC earthquake).

According to the focal mechanism solutions provided by published references, 26 earthquakes are strike-slip events, two earthquakes are normal-faulting events and two earthquakes are reverse-faulting events. Details can be found in the Electronic Supplement.

For the other earthquakes whose magnitudes are less than 5.0, focal mechanism solutions cannot be obtained either from the Global CMT catalogue or from the literature. Nevertheless, the tectonics of the Sichuan–Yunnan area can help assess the focal mechanisms

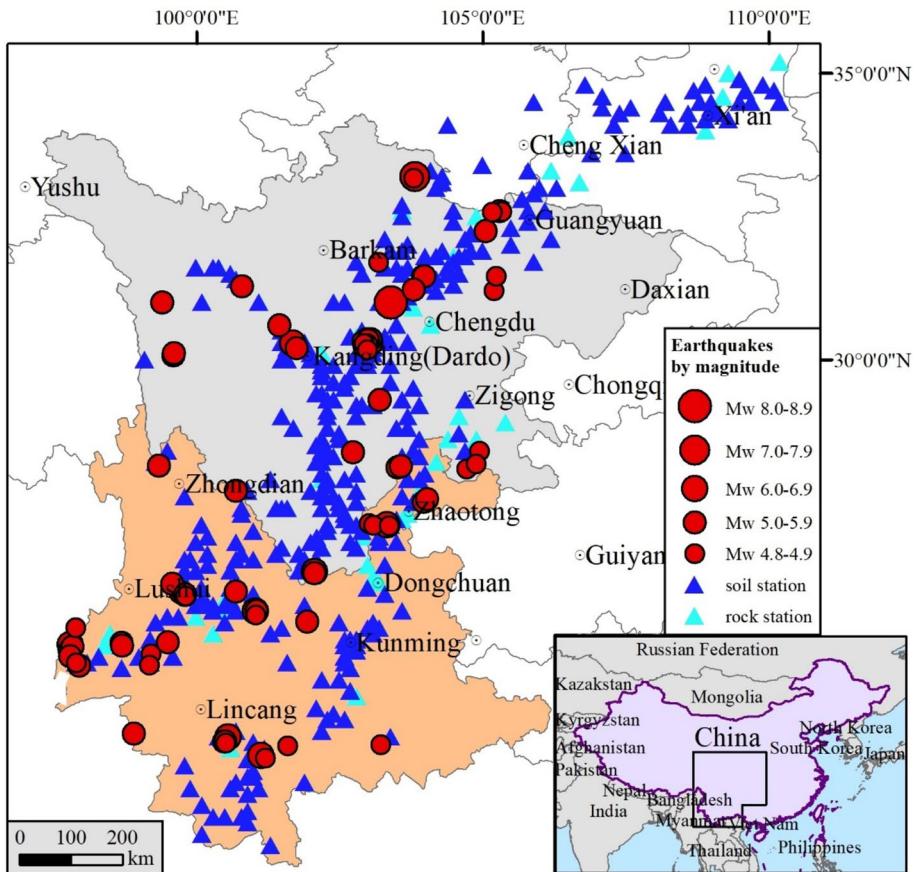


Fig. 3 Map showing the epicentres of earthquakes used in the comparison and the locations of recording stations. The aftershocks of the WC earthquake are not plotted due to their large quantity. Light grey and light orange polygons indicate the Sichuan and Yunnan provinces, respectively

of these small earthquakes. The Indian plate is colliding with the Eurasian plate and is moving towards the northeast, which forces the Tibetan plateau to continue to move in an east–south–southeast direction (Yin and Harrison 2000), whereas the relatively stable Huanan block resists the escaping movement of the plateau as a rigid barrier (Zhang et al. 2010). As strain response, modern tectonics in the Sichuan–Yunnan area is dominated by movements of translation, rotation and uplift of secondary active blocks. These blocks are bounded by a series of strike–slip faults combining dip–slip components (Xu et al. 2003). Hence, the focal mechanisms of earthquakes occurred in the Sichuan–Yunnan area are dominated by strike–slip faulting, with only a few normal-faulting and reverse-faulting events, which are distributed in the west and northeast of this area, respectively (Hu et al. 2017).

In consequence, we assume strike–slip faulting when evaluating the GMPEs for M_w less than 7.0. All PGAs and PSAs available at very large magnitudes are from the reverse-faulting WC earthquake of M_w 7.9 so the GMPEs are evaluated for reverse faulting for this event.

3.2 Distance parameters

Rupture distance (R_{rup}) needed to be estimated since it is the distance measure used in our candidate GMPEs. Although it is difficult to obtain the rupture geometries for all events in our database, it still is obtainable for the larger earthquakes along well-mapped faults.

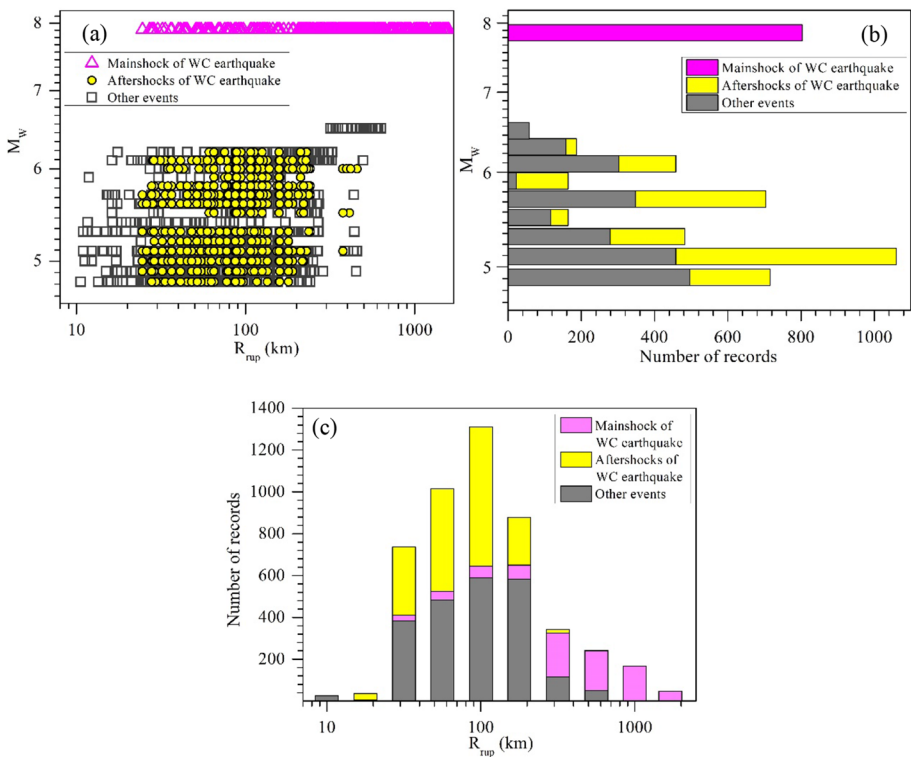


Fig. 4 **a** Magnitude–distance distribution of records, **b** distribution with magnitude, and **c** distribution with R_{rup}

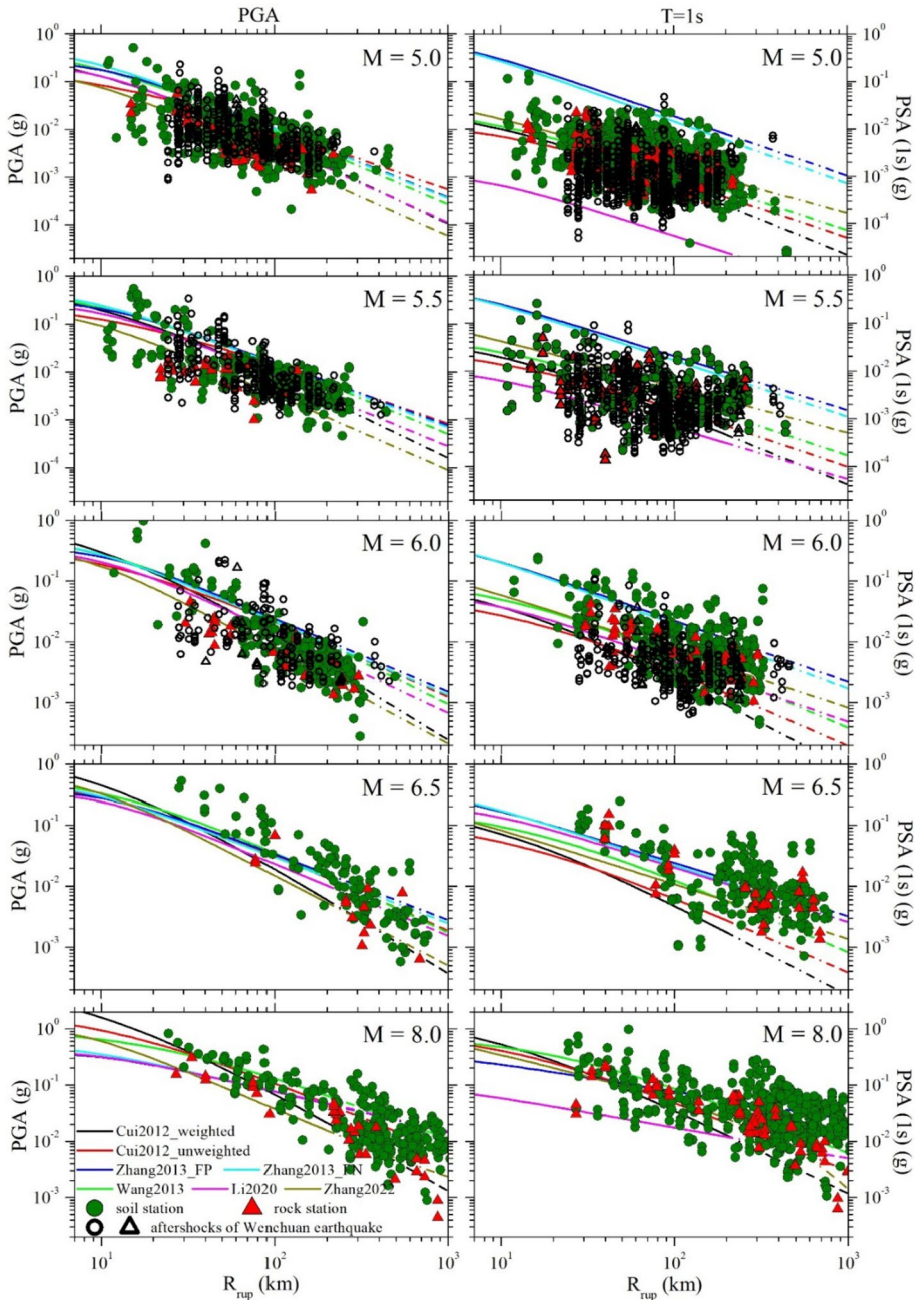


Fig. 5 Plots of observations and predictions for PGAs and PSAs (1s) against rupture distance for various magnitudes. For consistency amongst models, we show predictions for rock site conditions. According to the range of applicability of each GMPE listed in Table 2, the predictions are shown up to 200km with solid lines and beyond 200km with dash-dotted lines. Both Cui2012_weighted and Cui2012_unweighted are from Cui et al. (2012) but have different coefficients (this is the same for Zhang2013_FP and Zhang2013_FN)

Fig. 6 Variation of inter-event residuals against magnitude for PGA, PSA (0.1 s) and PSA (1 s). Black solid lines are linear fits, and the black dash lines indicate the 95% confidence intervals. Only the weighted model of Cui et al. (2012) and the FN model of Zhang et al. (2013) are presented here as their variants show similar results

We identified 30 earthquakes with sufficient information from which we could estimate rupture geometries (Electronic Supplement). For these earthquakes, estimates of R_{rup} for all stations were obtained using the estimated rupture geometries and the Fault-to-Station Distance program (Boore 2019). For the other 41 earthquakes with M_w less than 5 for which rupture geometries could not be identified, hypocentral distance (R_{hypo}) was used as a proxy distance measure. Most observations from earthquakes of $M_w \leq 5$ are recorded at 30–200 km from the rupture plane (Fig. 4a). Due to the likely small size of these ruptures (less than 5×5 km) the effect of this assumption will be negligible.

Figure 4c shows the number of records against R_{rup} . For all events, most records are in the distance range 30–300 km. For large earthquakes, and particularly the M_w 7.9 WC earthquake, records are also available from 300 to 1000 km. There are a large number of records from aftershocks of the WC earthquake, most of which are located at 30–200 km away [the magnitudes of these aftershocks are smaller than 6.2 and mainly range from 4.8 to 5.6].

3.3 Comparisons of GMPEs to local records

Zhang et al. (2013), Li et al. (2020) and Zhang et al. (2022) included terms to model the effect of different styles of faulting. For the strike-slip faulting events, the style-of-faulting term $f_{fit} = 0$. Cui et al. (2012) and Wang et al. (2013) did not include style-of-faulting terms. These three GMPEs (Zhang et al. 2013, 2022; Li et al. 2020) also included hanging-wall terms. The hanging wall effect can sometimes be observed in the near-source area ($R \leq 40$ km) at short spectral periods (e.g., Abrahamson and Somerville 1996). In the Sichuan–Yunnan area, most faults have strike-slip mechanisms with high dip angles. In addition, most records are located more than 30 km from the rupture plane (Fig. 4c), so hanging-wall effects would likely be minimal in the vast majority of cases. Hence, we did not use the hanging-wall terms. All GMPEs used V_{S30} in their site-effect term except that by Wang et al. (2013). Average V_{S30} of 553 m/s and 353 m/s (Yu et al. 2016) are assumed for rock and soil sites, respectively.

We plotted the predicted values from the candidate GMPEs (Cui et al. 2012; Wang et al. 2013; Zhang et al. 2013, 2022; Li et al. 2020) and observed values for PGA and PSA (1 s) against rupture distance (R_{rup}) for various magnitudes. We used a magnitude bin of ± 0.2 around the central value to group the observations for each magnitude interval. For PGAs from all considered magnitudes, there is a good match between predictions and observations from rock stations at all distances, especially from 30 to 200 km (Fig. 5). Overall, the predictions of PGAs fit the observations from soil stations as well, especially for $M_w = 5.0, 5.5$ and 6.0. Furthermore, the plots for the WC aftershocks show the same pattern. For $M_w = 6.5$, the predictions for PGA are slightly lower than the observations from soil stations but this is based on limited records.

For period 1s, the predictions from GMPEs show wider fluctuation, and the smaller magnitudes ($M_w = 5.0, 5.5$ and 6.0) show wider dispersion amongst GMPEs. The predictions generally match the observations from both rock and soil stations well. For $M_w = 6.5$ and 8.0, some predictions are slightly lower than the observations from soil

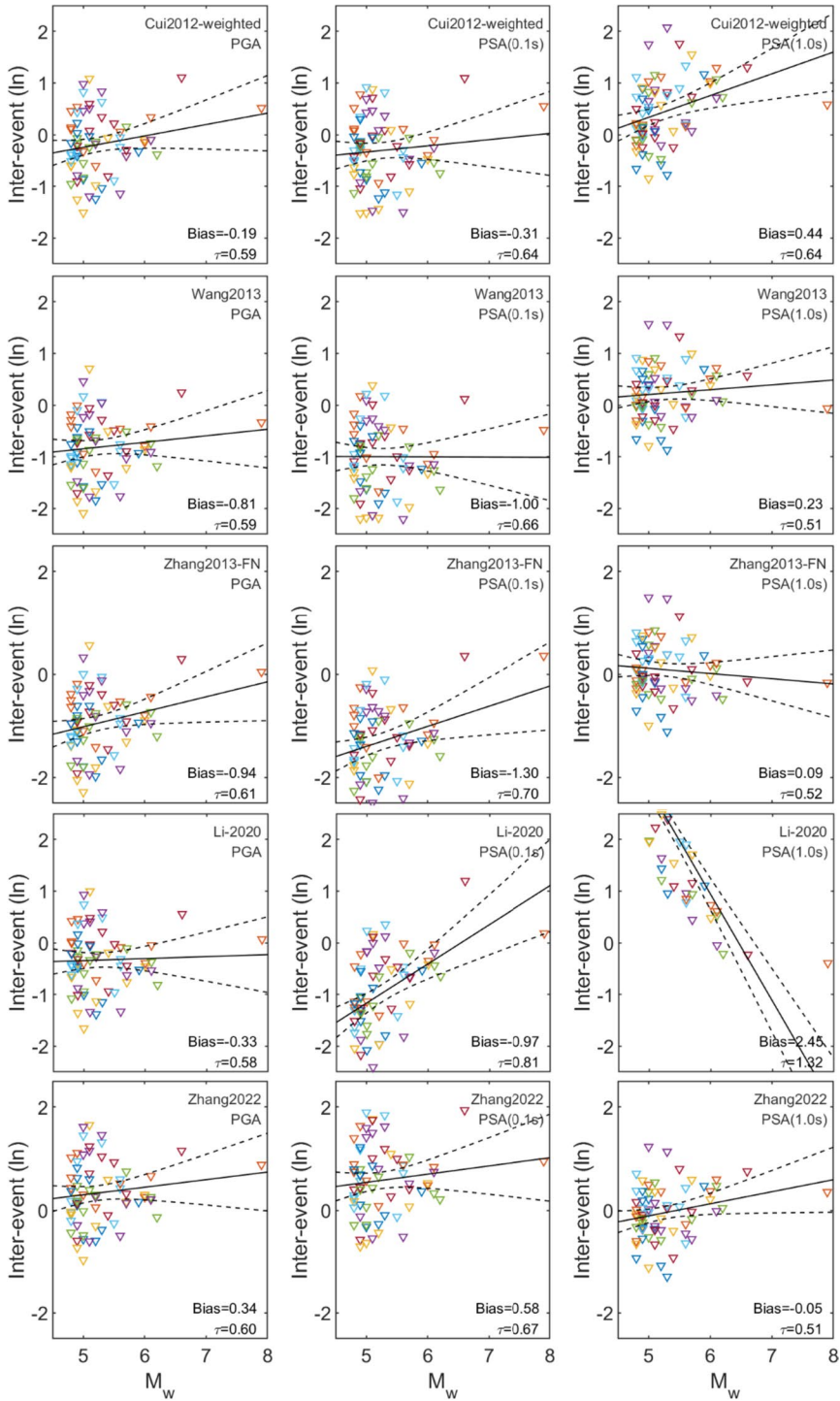


Fig. 7 Variation of intra-event residuals against rupture distance for PGA, PSA (0.1 s) and PSA (1 s). Black solid lines are linear fits, and black dash lines indicate the 95% confidence intervals. Green and red circles indicate records from soil and rock stations, respectively

stations but most under-predictions happen for records from more than 200km. For the WC aftershocks, more observations are under-predicted and the observations are marginally lower than those from mainshocks for the same magnitude. This finding is consistent with previous studies (e.g., Douglas and Halldórsson 2010).

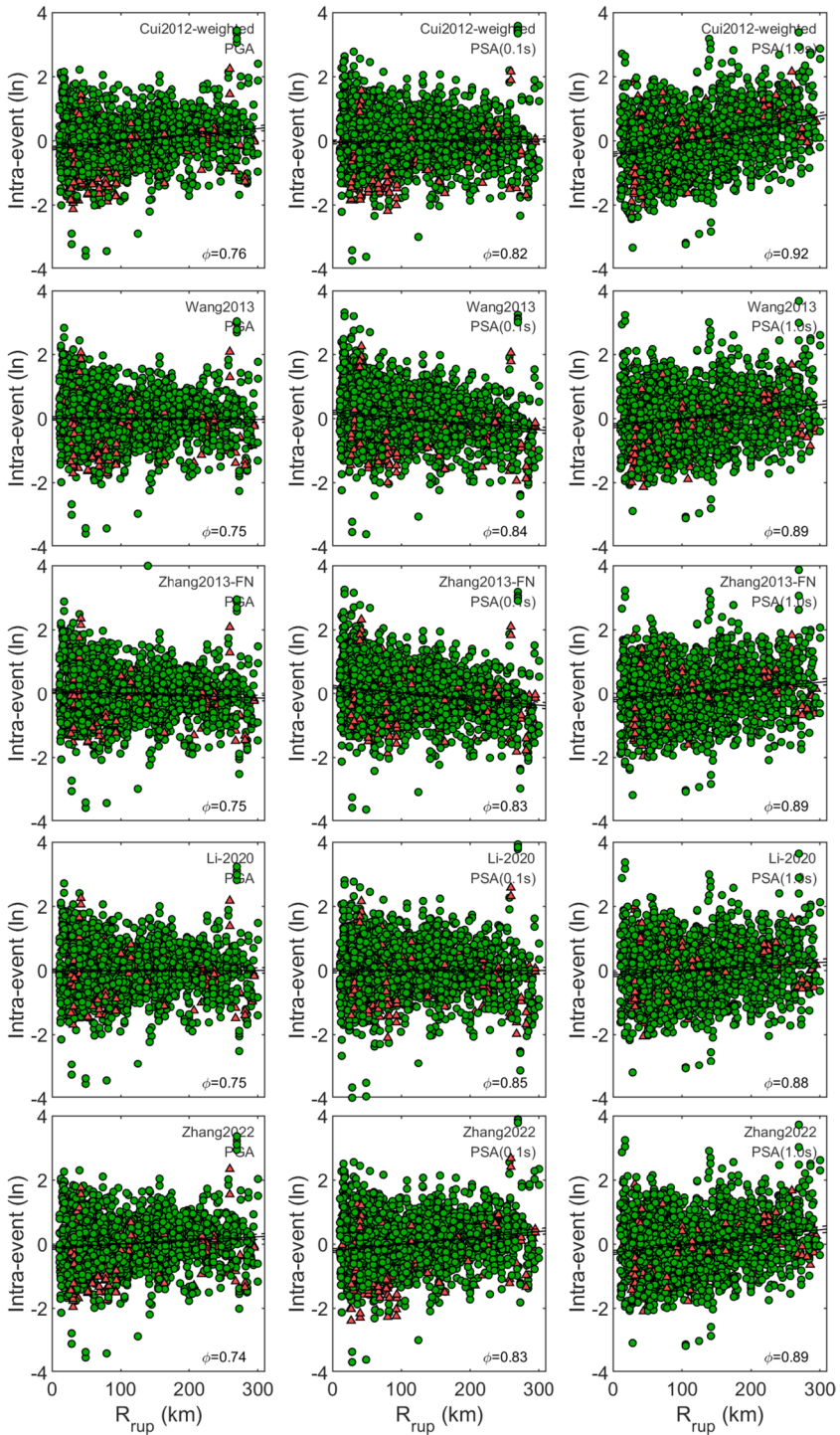
The inter- and intra-event residuals are computed using the algorithm of Abrahamson and Youngs (1992). The residual analysis is restricted to the data from within $R_{rup} = 300$ km, which is the farthest distance considered in most seismic hazard analyses. This means 2,469 records (70 events) are included.

The magnitude scaling is tested by plotting inter-event residuals against magnitude. The results in Fig. 6 indicate mixed findings with respect to the misfit between the magnitude-scaling of the candidate GMPEs and local observations. The inter-event (tau) standard deviations range from 0.5 to 0.7, which are larger than commonly-observed values of about 0.3–0.5 (e.g., Douglas and Edwards 2016). The results suggest that ground motions from earthquakes in the Sichuan–Yunnan area are more variable than those in other regions.

To clearly understand the variation of inter-event residuals with magnitude, we derived linear best-fit lines from the residuals. The slope of the line, namely the trend, indicates a mismatch in the magnitude-scaling of the model and the data. The residuals from Cui et al. (2012) show strong trends against magnitude for PSA at 1s, while for PGA and PSA at 0.1 s the trends are less clear. The relatively low means of the inter-event residuals (biases) and the weak trends in the inter-event residuals with respect to magnitude show that this model can predict PGA and PSA (0.1 s) better than PSA (1 s). Wang et al. (2013) has high bias for PGA and PSA (0.1 s), suggesting a large misfit between predictions and observations, while the model could generate good predictions for PSA (1 s). The trends for Wang et al. (2013) are weak for all presented periods, especially at 0.1 s. Zhang et al. (2013) also shows better predictions for PSA (1 s), as indicated by lower bias and weaker trends for this response period. For PGA and PSA (0.1 s), however, the misfit between predictions and observations are obvious as the biases are high. For Li et al. (2020), there is a weak trend for PGA but the trends for PSA (0.1 s) and PSA (1 s) are extremely strong. Zhang et al. (2022) shows better behaviour for PGA and PSA (1 s) than for PSA (0.1 s), but compared to other models, it provides relatively good predictions for PGA and PSA at both 0.1 s and 1 s. There are trends for PGA, PSA (0.1 s) and PSA (1 s) but all of them are slight and show the same overall pattern.

As shown in Fig. 6, most GMPEs produced better predictions for earthquakes with magnitude between 5.5 and 6.5 but the predictions from Cui et al. (2012) and Zhang et al. (2022) show a clear misfit at $M_w = 6.6$ (the Lushan earthquake in 2013), with the inter-event residual for this event being much greater than zero for these two GMPEs. However, it is hard to conclude whether any of the GMPEs can provide good predictions for all strong earthquakes due to the limited records from this magnitude range.

The distance scaling is tested by examining the intra-event residuals versus R_{rup} . As shown in Fig. 7, all models generally indicate small biases and trends in terms of their distance scaling for PGA. Most models indicate weak trends for PSA at 0.1 s and 1 s as well. Wang et al. (2013) and Zhang et al. (2013) show trends for PSA (0.1 s) and



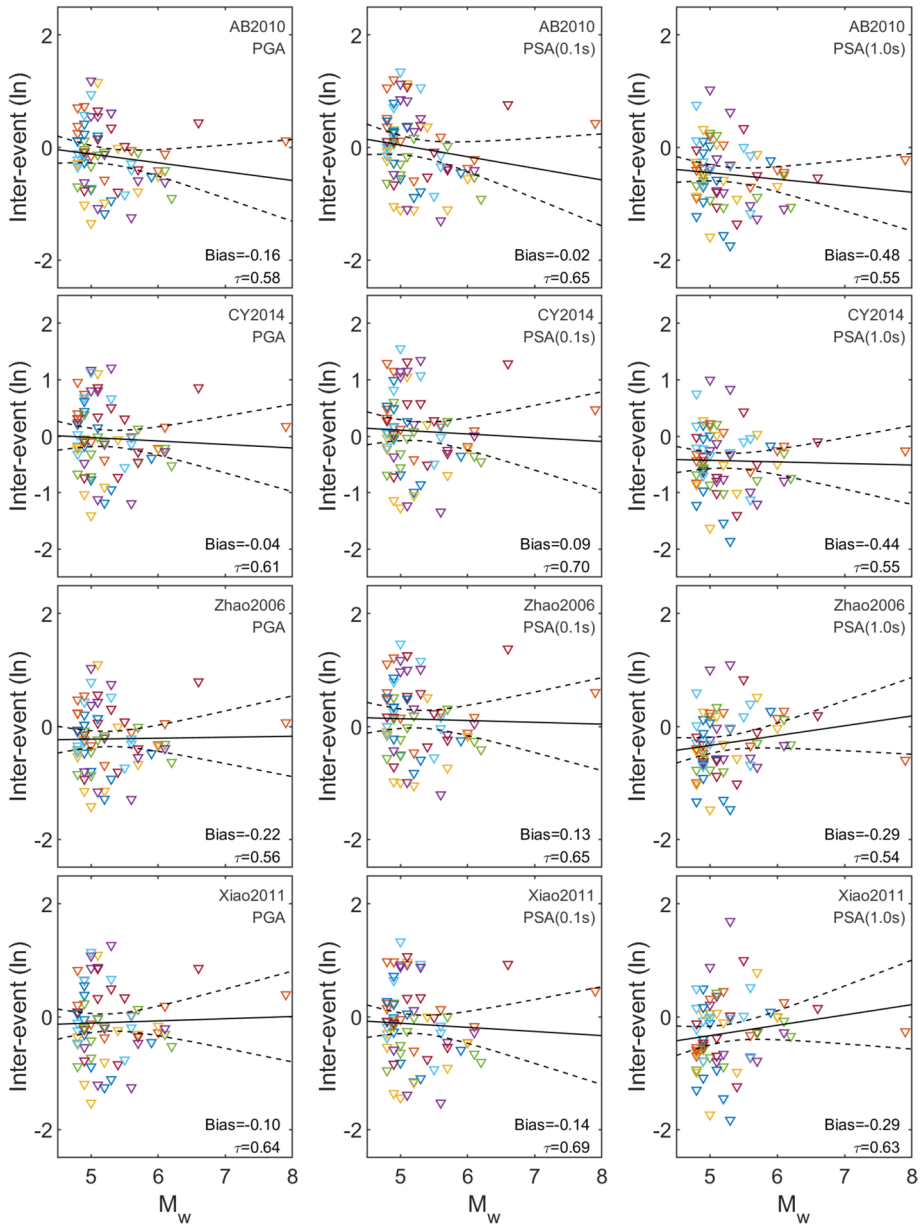


Fig. 8 Variation of inter-event residuals against magnitude for PGA, PSA (0.1 s) and PSA (1 s) for three global and one Chinese GMPE. Black solid lines are linear fits, and the black dash lines indicate its 95% confidence intervals. CEA (2019) is updated from Xiao (2011) so it shares the same functional form and the coefficients for response periods from 0 to 1.2 s with Xiao (2011). Due to all periods considered in our analysis being less than 1.2 s, we only present the results for Xiao (2011) for the major axis, although predictions for the minor axis are similar

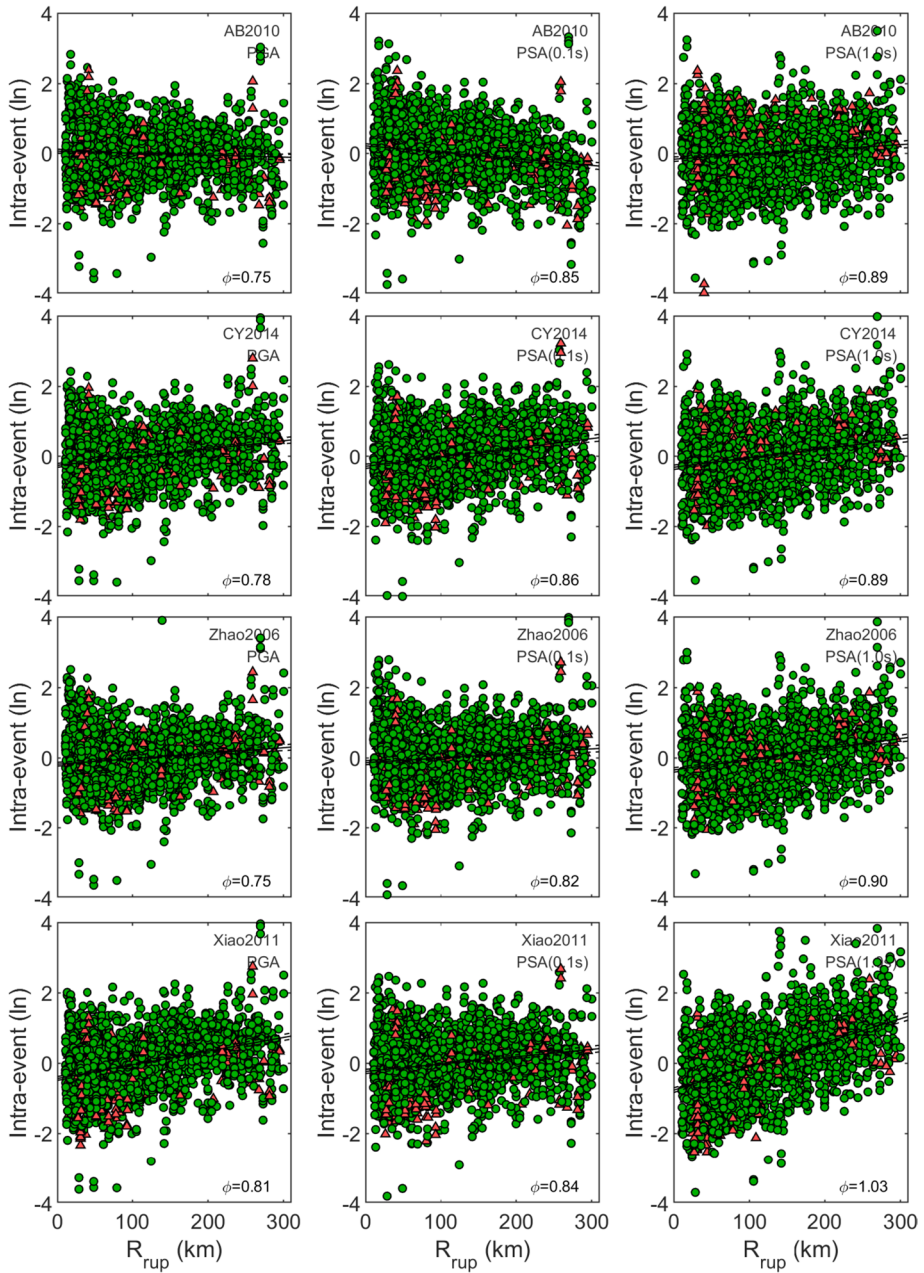


Fig. 9 Variation of intra-event residuals against rupture distance for PGA, PSA (0.1 s) and PSA (1 s) for three global and one Chinese GMPE. Black solid lines are linear fits, and black dash lines indicate its 95% confidence intervals. Green and red circles indicate records from soil and rock stations, respectively

Cui et al. (2012) shows a relatively stronger trend for PSA (1 s). Overall, Zhang et al. (2022) shows a good performance against distance that for all considered spectral periods. The weak trends mainly occur at distances beyond 200 km, which is beyond this model's reported range of applicability. The results also indicate that all models show weaker trends for PGA and short periods than longer periods.

3.4 Comparisons with another widely used and recommended GMPEs

We have also compared worldwide GMPEs to local ground-motion records. For active shallow crustal regions, three empirical models, AB2010 (Akkar and Bommer 2010), CY2008 (Chiou and Youngs 2008), and Zhao2006 (Zhao et al. 2006), were recommended for the Global Earthquake Model by Stewart et al. (2015). Chiou and Youngs (2008) has been updated to Chiou and Youngs (2014) during the NGA-West2 project. The new version is also recognized as an adaptable GMPE for active crustal regions (Bommer and Stafford 2020). Therefore, we adopted CY2014 (Chiou and Youngs 2014) rather than 2008 version. In addition, as the most widely used GMPEs in China, Xiao (2011) and CEA (2019) were also included in the comparison.

The results in Fig. 8 indicate low bias and no strong trends in the plots for inter-event residuals, which suggests that the three worldwide GMPEs and the two widely-used Chinese GMPEs provide good predictions for the local data, particularly for PGA and PSA (0.1 s). The inter-event (τ) standard deviation remains large. The bias for PSA (1.0 s) and trends are slightly higher but still better than most of the local GMPEs.

The plot of intra-event residuals against distance shown in Fig. 9 indicates that the three worldwide GMPEs display slight trends with respect to their distance attenuation for PGA and PSA at 0.1 s and 1.0 s. The two Chinese GMPEs show strong trends, especially for PSA (1.0 s), which are worse than those observed for the local GMPEs.

Perhaps surprisingly, the worldwide GMPEs present better compatibility to the local data than the local GMPEs. The NGA-West2 model (CY2014) shows the best prediction in terms of magnitude and distance scaling and overall ground-motion levels.

The results also suggest that the source characteristics of earthquakes in the Sichuan–Yunnan area are more variable than in other regions because of the larger inter-event standard deviations. This could be explained by the complicated tectonic characteristics, which may also have led to the seismic hazard of this area being underestimated by the Chinese zonation map. The results indicate that using only local GMPEs may not be appropriate when estimating the seismic hazard of this area. The combined use of local models and robust global models within a GMM, potentially composed of equally-weighted predictions from the Zhang et al. (2022), Akkar and Bommer (2010), Chiou and Youngs (2014), Zhao et al. (2006) and CEA (2019) GMPEs, would be more appropriate.

4 Conclusions and recommendations

In this article, we evaluated local GMPEs for the Sichuan–Yunnan area based on their characteristics as well as by comparing them with local ground-motion data. From the local GMPEs, that by Zhang et al. (2022) is considered the best for the area. Several reasons support this conclusion: a good and accessible dataset, a standard functional form than captures the main magnitude- and distance-scaling effects, and a good match

to the local ground-motion data. Our results also indicate that the distance attenuation of Zhang et al. (2022) matches the observations better than the widely-used GMPEs in China by Xiao (2011) and CEA (2019). Therefore, we recommend the Zhang et al. (2022) GMPE for use within seismic hazard analyses for engineering projects.

Although the rapidly increasing number of seismic stations in China enables the development of local GMPEs, some new local GMPEs suffer from problems, such as poor dataset selection, insufficient consideration of site effects and unusual functional forms. In addition, due to the relatively short recording history, the datasets used to derive the GMPEs does not cover the entire magnitude range of interest for seismic hazard analyses, especially at large magnitudes ($M > 6.5$). Hence, the local GMPEs for the Sichuan–Yunnan area, and potentially also for the whole of China, could be improved in several ways. For example, rather than deriving completely new models, local GMPEs could be developed by adjusting robust GMPEs from elsewhere. Based on our analysis using local ground-motion data, global GMPEs generally show better performance than local models. The results also suggest that improved estimates of V_{S30} for seismic stations could help to decrease the uncertainty associated with ground-motion prediction. Finally, the results suggest that earthquake ground motions in the Sichuan–Yunnan area are more variable than those in other active crustal regions.

Supplementary Information The online version contains supplementary material available at <https://doi.org/10.1007/s10518-024-01861-9>.

Acknowledgements The authors thank Yi Du and Jingyi Zhao at the National Institute of Natural Hazards, Ministry of Emergency Management of China for providing the ground-motion data. We thank Alireza Azarbakht and an anonymous reviewer for their detailed comments on a previous version of this manuscript, which led to significant improvements.

Author contributions Both authors contributed to the study conception and design. Material preparation and data collection were performed by Jingwei Liu. Analysis was performed by Jingwei Liu and John Douglas. The first draft of the manuscript was written by Jingwei Liu. John Douglas edited this draft. Both authors read and approved the final manuscript. Both authors undertook the revisions to the manuscript.

Funding This work was undertaken during Jingwei Liu's visit at the Department of Civil and Environmental Engineering, University of Strathclyde, which was funded by the China Scholarship Council (No. 202004190043).

Data Availability Ground-motion data were provided by the Strong Motion Observation Centre, Institute of Engineering Mechanics, China Earthquake Administration.

Declarations

Competing interests The authors have no relevant financial or non-financial interests to disclose.

Open Access This article is licensed under a Creative Commons Attribution 4.0 International License, which permits use, sharing, adaptation, distribution and reproduction in any medium or format, as long as you give appropriate credit to the original author(s) and the source, provide a link to the Creative Commons licence, and indicate if changes were made. The images or other third party material in this article are included in the article's Creative Commons licence, unless indicated otherwise in a credit line to the material. If material is not included in the article's Creative Commons licence and your intended use is not permitted by statutory regulation or exceeds the permitted use, you will need to obtain permission directly from the copyright holder. To view a copy of this licence, visit <http://creativecommons.org/licenses/by/4.0/>.

References

- Abrahamson NA, Somerville PG (1996) Effects of the hanging wall and footwall on ground motions recorded during the Northridge earthquake. *Bull Seismol Soc Am* 86(1B):S93–S99
- Abrahamson NA, Youngs RR (1992) A stable algorithm for regression analyses using the random effects model. *Bull Seismol Soc Am* 82(1):505–510
- Abrahamson NA, Atkinson GM, Boore DM, Bozorgnia Y, Campbell KW, Chiou BS, Idriss IM, Silva WJ, Youngs RR (2008) Comparisons of the NGA ground-motion relations. *Earthq Spectr* 24(1):45–66
- Akkar S, Bommer JJ (2010) Empirical equations for the prediction of PGA, PGV and spectral accelerations in Europe, the Mediterranean region and the middle east. *Seismol Res Lett* 81:195–206. <https://doi.org/10.1785/gssrl.81.2.195>
- Al Atik L, Abrahamson N, Bommer JJ, Scherbaum F, Cotton F, Kuehn N (2010) The variability of ground-motion prediction models and its components. *Seismol Res Lett* 81(5):794–801. <https://doi.org/10.1785/GSSRL.81.5.794>
- Bommer JJ, Stafford P (2020) Selecting ground-motion models for site-specific PSHA: adaptability versus applicability. *Bull Seismol Soc Am* 110(6):2801–2815
- Bommer JJ, Douglas J, Scherbaum F, Cotton F, Bungum H, Fäh D (2010) On the selection of ground-motion prediction equations for seismic hazard analysis. *Seismol Res Lett* 81(5):783–793. <https://doi.org/10.1785/gssrl.81.5.783>
- Boore D (2019) Fault-to-Station distance program. https://www.daveboore.com/software_online.html
- Campbell KW (2016) Comprehensive comparison among the Campbell–Bozorgnia NGA-West2 GMPE and three GMPEs from Europe and the middle east. *Bull Seismol Soc Am* 106(5):2081–2103. <https://doi.org/10.1785/0120160024>
- Campbell KW, Bozorgnia Y (2006) Next generation attenuation (NGA) empirical ground motion models: Can they be used in Europe?. In: *Proceeding of 1st European conference on earthquake engineering and seismology*, Geneva, Switzerland, 3–8 September 2006, Paper Number 458
- Cheng J, Rong Y, Magistrale H, Chen G, Xu X (2017) An Mw-based historical earthquake catalog for Mainland China. *Bull Seismol Soc Am* 107(5):2490–2500. <https://doi.org/10.1785/0120170102>
- China Earthquake Administration (CEA) (2019) Outline for regional seismic hazard assessment projects (trial version). China Earthquake Administration, Beijing (in Chinese)
- Chiou BS, Youngs RR (2008) An NGA model for the average horizontal component of peak ground motion and response spectra. *Earthq Spectr* 24(1):173–215
- Chiou BS, Youngs RR (2014) Update of the Chiou and Youngs NGA model for the average horizontal component of peak ground motion and response spectra. *Earthq Spectr* 30(3):1117–1153
- Cotton F, Scherbaum F, Bommer JJ, Bungum H (2006) Criteria for selecting and adjusting ground-motion models for specific target applications: applications to Central Europe and rock sites. *J Seismol* 10(2):137–156
- Cui J, Li S, Gao D, Zhao Y, Bao Y (2006) Ground motion attenuation relation in the Yunnan area. *J Seismol Res* 29(4):386–391 (in Chinese)
- Cui J, Zhang J, Gao D, Duan J, Wang T (2012) The ground motion attenuation relation for the mountainous area in Sichuan and Yunnan. In: *Proceedings of the 15th world conference on earthquake engineering*, Lisbon
- Douglas J (2003) Earthquake ground motion estimation using strong-motion records: a review of equations for the estimation of peak ground acceleration and response spectral ordinates. *Earth Sci Rev* 61(1–2):43–104
- Douglas J, Edwards B (2016) Recent and future developments in earthquake ground motion estimation. *Earth Sci Rev* 160:203–219
- Douglas J (2018) Capturing geographically-varying uncertainty in earthquake ground motion models or what we think we know may change. In: Pitilakis, K. (eds) *Recent advances in earthquake engineering in Europe*. ECEE 2018. Geotechnical, geological and earthquake engineering, vol 46. Springer, Cham
- Douglas J, Halldórsson B (2010) On the use of aftershocks when deriving ground-motion prediction equations. In: *Proceedings of the 9th U.S. National and 10th Canadian conference on earthquake engineering*. Paper no. 220.
- Fan W, Du W, Wang X, Shao H, Wen Y (2011) Seismic motion attenuation relations in Shanxi areas. *J Earthq Eng Eng Vib* 31(2):47–54 (in Chinese)
- Fan Z, Tang Q, Xu R, Liu J (2020) Attenuation of horizontal earthquake ground motion in the southern segment of the North-South Seismic Belt, China. *Chin J Geophys* 63(1):223–235 (in Chinese)
- Ghasemi H, Allen T (2022) Selection of ground-motion models for national seismic hazard assessment of Australia. In: *Australian earthquake engineering society 2022 national conference*, 24–25 November 2022 Mount Macedon, Victoria, Australia

- Goulet C, Bozorgnia Y, Abrahamson NA, Kuehn N, Al Atik L, Youngs RR, Graves R (2018) Central and Eastern North America Ground-Motion Characterization—NGA-East Final Report (PEER 2018/08). Pacific Earthquake Engineering Research Center, University of California, Berkeley
- Gregor N, Addo K, Abrahamson NA, Atik LA, Atkinson GM, Boore DM, Bozorgnia Y, Campbell KW, Chiou BS, Gulerce Z, Hassani B, Kishida T, Kuehn N, Mazzoni S, Midorikawa S, Parker GA, Si H, Stewart JP, Youngs RR (2022) Comparisons of the NGA-Subduction ground motion models. *Earthq Spectr* 38(4):2580–2610
- Hu Y, Zhang M (1984) A method of predicting ground motion parameters for regions with poor ground motion data. *J Earthq Eng Eng Vib* 4(1):1–11 (in Chinese)
- Hu X, Zang A, Heidhach O, Cui X, Xie F, Chen J (2017) Crustal stress pattern in China and its adjacent areas. *J Asian Earth Sci* 149:20–28. <https://doi.org/10.1016/j.jseaeas.2017.07.005>
- Huang C, Galasso C (2019) A comparison of NGA-West2 ground-motion models to recent Chinese data. *Soil Dyn Earthq Eng* 125:105677
- Huo J (1989) Study on the attenuation law of near field ground motion. Dissertation, Institute of Engineering Mechanics, State Seismological Bureau (in Chinese)
- Jiang Y (2017) The ground motion model of small and medium earthquakes in Sichuan area considering different site classification. Thesis: Institute of Engineering Mechanics, China Earthquake Administration (in Chinese)
- Kale O, Akkar S (2013) A new procedure for selecting and ranking ground-motion prediction equations (GMPEs): the Euclidean distance-based ranking (EDR) method. *Bull Seismol Soc Am* 103(2A):1069–1084
- Kang L, Jin X (2009) Ground motion attenuation relations of small and moderate earthquakes in Sichuan region. *Earthq Sci* 22:277–282
- Lanzano G, Luzi L, Amico VD, Pacor F, Meletti C, Marzocchi W, Rotondi R, Varini E (2020) Ground motion models for the new seismic hazard model of Italy (MPS19): selection for active shallow crustal regions and subduction zones. *Bull Earthq Eng* 18:3487–3516. <https://doi.org/10.1007/s10518-020-00850-y>
- Lei J, Gao M, Yu Y (2007) Seismic motion attenuation relations in Sichuan and adjacent areas. *Acta Seismol Sin* 29(5):500–511 (in Chinese)
- Li X, Zhai C, Wen W, Xie L (2020) Ground motion prediction model for horizontal PGA, 5% damped response spectrum in Sichuan–Yunnan region of China. *J Earthq Eng* 24(11):1829–1866. <https://doi.org/10.1080/13632469.2018.1485600>
- McNamara DE, Petersen MD, Thompson EM, Powers PM, Shumway AM, Hoover SM, Moschetti MP, Wolin E (2019) Evaluation of ground-motion models for USGS seismic hazard forecasts: induced and tectonic earthquakes in the central and eastern United States. *Bull Seismol Soc Am* 109(1):322–335
- Ministry of Housing and Urban-Rural Development of the People’s Republic of China (MHUDPRC) (2010) Code for seismic design of buildings (GB5001–2010).
- Mousavi M, Ansari A, Zafarani H, Azarbakht A (2012) Selection of ground motion prediction models for seismic hazard analysis in the Zagros region, Iran. *J Earthq Eng* 16:1184–1207
- Mousavi M, Zafarani H, Rahpeyma S, Azarbakht A (2014) Test of goodness of the NGA ground-motion equations to predict the strong motions of the 2012 Ahar–Varzaghan dual earthquakes in northwestern Iran. *Bull Seismol Soc Am* 104(5):2512–2528
- Scasserra G, Stewart JP, Bazzurro P, Lanzo G, Mollaioli F (2009) A comparison of NGA ground-motion prediction equations to Italian data. *Bull Seismol Soc Am* 99:2961–2978
- Scherbaum F, Cotton F, Smit PM (2004) On the use of response spectral-reference data for the selection and ranking of ground motion models for seismic hazard analysis in regions of moderate seismicity: the case of rock motion. *Bull Seismol Soc Am* 94(6):2164–2184
- Scherbaum F, Delavaud E, Riggelsen C (2009) Model selection in seismic hazard analysis: an information-theoretic perspective. *Bull Seismol Soc Am* 99(6):3234–3247
- Stafford PJ, Strasser FO, Bommer JJ (2008) An evaluation of the applicability of the NGA models to ground-motion prediction in the Euro-Mediterranean region. *Bull Earthq Eng* 6:149–177
- Stewart JP, Douglas J, Javanbarg M, Bozorgnia Y, Abrahamson NA, Boore DM, Campbell KW, Delavaud E, Erdik M, Stafford PJ (2015) Selection of ground motion prediction equations for the global earthquake model. *Earthq Spectr* 31(1):19–45
- Wang S, Yu Y, Gao A, Yan X (2000) Development of attenuation relations for ground motion in China. *Earthq Res China* 16(2):99–106 (in Chinese)
- Wang Y, Li X, Zhou Z (2013) Research on attenuation relationships for horizontal strong ground motions in Sichuan–Yunnan region. *Acta Seismol Sin* 35(2):238–249. <https://doi.org/10.3969/J.ISSN.0253-3782.2013.02.010>

- Wang Y (2010) Analyses of strong ground motion intensity and its characteristics. Dissertation: Institute of Engineering Mechanics, China Earthquake Administration (in Chinese)
- Weatherill G, Kotha SR, Cotton F (2020) A regionally-adaptable “scaled backbone” ground motion logic tree for shallow seismicity in Europe: application to the 2020 European seismic hazard model. *Bull Earthq Eng* 18:5087–5117
- Wen R, Xu P, Wang H, Ren Y (2018) Single-station standard deviation using strong-motion data from Sichuan region, China. *Bull Seismol Soc Am* 108(4):2237–2247. <https://doi.org/10.1785/0120170276>
- Xiao L (2011) Study on the attenuation relationships of horizontal ground motion parameters near the source of rock site. Dissertation, Institute of Geophysics, China Earthquake Administration (in Chinese)
- Xu X, Wen X, Zheng R, Ma W, Song F, Yu G (2003) Pattern of latest tectonic motion and its dynamics for active blocks in Sichuan–Yunnan region, China. *Sci China Earth Sci* 46:210–226
- Yin A, Harrison TM (2000) Geologic evolution of the Himalayan–Tibetan orogen. *Annu Rev Earth Planet Sci* 28:211–280
- Yu Y, Wang S (2004) Attenuation relations for horizontal peak ground acceleration and response spectrum in northeastern Tibetan plateau region. *Acta Seismol Sin* 26(6):591–600 (in Chinese)
- Yu Y, Wang S (2006) Attenuation relations for horizontal peak ground acceleration and response spectrum in eastern and western China. *Technol Earthq Disast Prevent* 1(3):206–217 (in Chinese)
- Yu Y, Silva WJ, Darragh B, Li X (2016) V_{s30} estimate for southwest China. *Int J Geophys* 2016:9305095
- Yu Y (2002) Study on attenuation relationships of long period ground motions. Dissertation, Institute of Geophysics, China Earthquake Administration (in Chinese)
- Zhang Z, Yuan X, Chen Y, Tian X, Kind R, Li X, Teng J (2010) Seismic signature of the collision between the east Tibetan escape flow and the Sichuan basin. *Earth Planet Sci Lett* 292:254–264
- Zhang Q, Hu J, Xie L, Jiang Z (2013) New generation ground motion attenuation model for western China. *J Tianjin Univ (Sci Technol)* 46(12):1079–1088
- Zhang B, Yu Y, Li X, Wang Y, Rong M (2021) Ground motion attenuation relationship of horizontal component of PGV and PGD in Southwest China. *Chin J Geophys* 64(8):2733–2748 (in Chinese)
- Zhang B, Yu Y, Li X, Wang Y (2022) Ground motion prediction equation for the average horizontal component of PGA, PGV, and 5% damped acceleration response spectra at periods ranging from 0.033 to 8.0s in southwest China. *Soil Dyn Earthq Eng* 159:107297. <https://doi.org/10.1016/j.soildyn.2022.107297>
- Zhao JX, Zhang J, Asano A, Ohno Y, Oouchi T, Takahashi T, Ogawa H, Irikura K, Thio HK, Somerville PG, Fukushima Y, Fukushima Y (2006) Attenuation relations of strong ground motion in Japan using site classification based on predominant period. *Bull Seismol Soc Am* 96(3):898–913
- Zhao F, Wang H, Zhang Y (2009) Study on attenuation relationship of horizontal acceleration response spectrum of moderate-small earthquakes for seismic safety evaluation of nuclear engineering. *Earthq Res China* 25(3):274–281

Publisher's Note Springer Nature remains neutral with regard to jurisdictional claims in published maps and institutional affiliations.